Renewable Energy and Power Quality Journal
https://repqj.com/index.php/repqj/index
RE&PQJ, Vol. 23, No. 6, 2025

Method for Locating Fault Points of Medium-Voltage Cables Based on Improved Wavelet Neural Network

Yibiao Huang[1,*], Wenxuan Xu[1], Yirong Ye[1], Xiaoqiang Wen[1], Xiong Chen[1], Yunxiang Xu[2]

[1]State Grid Fujian Fuzhou Electric Power Supply Company, State Grid Corporation of China, Fuzhou, 350004, Fujian Province, China
[2]NARI TECHNOLOGY CO., LTD, Nanjing, 211106, Jiangsu Province, China
[*]Corresponding author's email: huangyibiaodljcxm@163.com

Abstract. In view of the slow convergence and easy fall into local optimum of traditional WNN, this paper introduces wavelet basis adaptive selection and GA-PSO hybrid strategy to jointly tune the scaling factor, translation factor, weight, threshold and number of hidden nodes. First, the optimal wavelet basis is automatically selected by mutual information. Then, through GA global search and PSO local fine tuning, an improved WNN model is constructed and applied to medium voltage cable fault location. Simulation results show that under the condition of 100km cable, the improved WNN converges in 70 iterations, and the MAE and RMSE are reduced by 1.95km and 2.25km respectively compared with the traditional WNN, which significantly improves the positioning accuracy and convergence speed.

Key words. Medium voltage cable, Fault location, Wavelet neural network, GA-PSO algorithm, Adaptive wavelet basis

1. Introduction

Quickly and accurately locating cable faults is essential to assure the stable running of the power system [1,2]. Medium voltage cables have complex laying environments and are affected by factors such as temperature, humidity, and electromagnetic interference, resulting in complex fault modes [3,4]. Traditional fault location methods such as the TW (traveling wave) [5] and the impedance method [6] are affected by factors such as signal attenuation and noise interference when facing complex cable networks. In recent years, artificial intelligence technology, especially WNN(wavelet neural network), has been widely used in signal processing and pattern recognition. The traditional WNN training mainly relies on the gradient descent method, it easily falls into the local optimum, and the convergence speed is slow, which limits its practicality. How to improve the training algorithm of WNN, increase the fault signal characteristic extraction ability, and improve the fault localisation accuracy has already become an emergency problem to be addressed.

The aim of this paper is to construct an improved WNN-based fault point localisation method for medium voltage cables to increase the localisation accuracy and convergence speed in complex cable network environments. This paper introduces a MI(mutual information)-driven wavelet basis adaptive selection mechanism to automatically select the wavelet basis that best matches the current fault signal from multiple candidate wavelet bases, and integrates GA (Genetic Algorithm) and PSO (Particle Swarm Optimization). GA is used for global search and PSO is used for local fine adjustment to jointly optimize the hyperparameters of WNN, such as the scaling factor, translation factor, weight, threshold and number of hidden nodes. On this basis, the regularized MSE (Mean Squared Error) loss function and Adam optimization algorithm are introduced to further improve the network's training efficiency and generalization ability. The experiment was conducted under multiple different cable lengths, from 100km to 800km, and different noise conditions. The results show that the proposed method is significantly better than the traditional WNN and other intelligent algorithm models in terms of fault location accuracy. When the noise intensity is 5dB, the MAE(Mean Absolute Error) and RMSE(Root Mean Square Error) are 6.4km and 8.1km respectively, which are relatively low. It reaches the convergence state after 70 iterations, with good adaptability and convergence efficiency, which verifies the effectiveness and practicality of the improved WNN model in locating medium voltage cable fault points.

Contribution of the paper:

(1) This paper first introduces MI as an evaluation index to achieve automatic screening and matching of wavelet bases, significantly improving the ability of WNN to extract fault signal features and providing more accurate input features for fault location.

(2) The study combines the global search capability of GA with the local optimization capability of PSO to construct a GA-PSO(Genetic Algorithm-Particle Swarm

Optimization) hybrid optimization framework, and jointly optimizes key parameters of WNN such as scaling factor, translation factor, weight, threshold and number of hidden nodes, effectively overcoming the problem that traditional WNN is prone to fall into local optimality and slow convergence.

(3) The experiment was conducted under different cable lengths and different noise intensities. The results showed that the improved WNN model is superior to the traditional method in positioning accuracy and convergence efficiency, has good adaptability and practicality, and provides an innovative and effective technical path for fault diagnosis in complex environments of medium-voltage cables.

The rest of the paper is organized as follows: Section II reviews the existing cable fault location methods, including physical models and research based on neural networks and optimization algorithms, and analyzes their respective advantages and disadvantages. Section III elaborates on the WNN method based on MI-driven adaptive wavelet basis selection and GA-PSO hybrid optimization proposed in this paper to achieve joint tuning of scaling factor, translation factor, weight, threshold and number of hidden nodes. Section IV introduces the experimental design of medium voltage cable fault point location, including data acquisition, preprocessing and evaluation indicators. Section V shows the location results and convergence performance under different cable lengths and noise conditions, and compares multiple benchmark methods. Section VI discusses the experimental results and deeply analyzes the mechanism and algorithm advantages of each module. Section VII summarizes the full paper and points out the innovative contribution, application value and future research direction of the method.

2. Related Works

In the fault location of medium voltage cables, many scholars have adopted different schemes to study it, and have achieved a lot of research results, ensuring the safety of cables. Li S, Chen C and other scholars used the reflection coefficient spectrum and wave number domain reflection method to locate medium voltage cable faults, eliminating the influence of multiple reflections and locating ground faults more accurately. However, it is easily affected by signal attenuation in long-distance cables and branch cables, which reduces the positioning accuracy [7,8]. Sun G et al. applied the TW method to fault location of cables and other lines in medium voltage distribution networks, which improved the positioning accuracy to a certain extent. The results showed that the absolute error was less than 30 m. However, it relied on high-precision extraction of the arrival time of traveling waves, which made it difficult to cope with noise interference and dispersion [9]. Zeng R et al. built a new TW fault location solution based on the distance matrix and frequency-related TW velocity, which optimized the location accuracy. However, it was limited by the preset model parameters and lacked online self-calibration [10]. As a positioning method, the impedance method is used in the positioning of cable fault points. The fault point location is inferred by measuring the changes in cable resistance, inductance, capacitance and other parameters, but it is highly dependent on cable parameters and is prone to failure in the case of multiple faults [11,12]. Scholars have used TW method, impedance method and other methods to improve positioning accuracy to a certain extent, but they are easily affected by noise in complex environments, resulting in poor positioning accuracy.

In recent years, many researchers have used artificial intelligence technology to improve cable fault location methods and establish a mapping relationship between fault features and fault distances. Wan Q, Niaki S H A and other scholars used DBN (Deep Belief Network) and ANN (artificial neural network) to locate cable faults, which improved the feature extraction capability in fault location, but performed poorly under signal interference [13,14]. Hadaeghi A combined wavelet transform and artificial neural network to build WNN, and applied it to transmission line fault location, reducing the fault location error to 0.0045%. However, its training relies on gradient descent, the initial parameters are sensitive, the convergence is slow, and it is easy to fall into the local optimum [15]. Shang Z and other scholars used the time-frequency analysis and self-learning capabilities of WNN to diagnose faults, and performed well in signal feature extraction [16]. Scholars have applied WNN to fault location, which has improved the signal processing effect. However, the parameter initialization and optimization of WNN rely on the traditional gradient descent algorithm, which has a slow convergence speed and low accuracy.

Researchers have combined optimization algorithms to improve neural network methods, such as genetic algorithms, to optimize the weights and structure of neural networks and improve fault location accuracy. As a kind of optimization algorithm, GA algorithm is used to optimize the weights and thresholds of the positioning model combined with wavelet transform and BP neural network, which greatly reduces the positioning error, but the convergence speed is slow [17,18]. In the fault location of distribution network, Zhou C and other scholars used GA algorithm for parameter optimization of BPNN (back propagation neural network) model and output better parameters. However, pure GA search lacks local refinement ability and the fitness function is easily disturbed by noise [19]. In denoising, PSO is used to adjust the network parameters of WNN. It enhances the ability to suppress noise and performs well in local search, but is prone to premature convergence problems [20]. Ong P et al. used CSA (cuckoo search algorithm) to optimize the parameters of WNN such as hidden nodes and initial positions. The results showed that it has better generalization ability than a single WNN, but its convergence path also lacks diversified guarantees and is difficult to cope with multi-modal fault characteristics [21]. The above scholars use GA or PSO alone to optimize WNN, which has the risk of slow convergence or premature convergence, and poor network parameter optimization ability. Existing research mostly relies on

manual experience in the selection of wavelet basis, lacks adaptive adjustment mechanism, and there is a large research gap in the field of cable fault location.

Current research on cable fault location mainly focuses on two types of methods: traveling wave method and impedance method based on the physical characteristics of electrical signals, and neural network method based on artificial intelligence. The TW method and its improvements such as reflection coefficient spectrum and dispersion correction have high accuracy in short distances or simple topologies, but are highly dependent on accurate extraction of traveling wave arrival times, are sensitive to noise and cable dispersion, and are difficult to maintain stability in long distances, multiple branches or complex environments. The impedance method has an intuitive advantage in parameter measurement, but its strong dependence on line electrical parameters leads to rapid failure when multiple faults or parameter estimation errors exist. Although deep models such as DBN and ANN combined with WNN and wavelet preprocessing have improved the ability to extract nonlinear features, they are difficult to meet the needs of real-time and high-precision fault location because of their dependence on gradient descent for training, sensitivity to initial parameters, slow convergence, and easy to fall into local optimality.

Scholars have introduced optimization algorithms such as GA, PSO, and CSA to perform global or local searches on neural network parameters. Although the convergence performance and noise suppression have been improved to a certain extent, a single algorithm often cannot take into account both global exploration and local refinement. Although GA search is comprehensive, it converges slowly, PSO is fast but prone to premature maturity, and CSA has limited diversity. Existing WNN research generally uses fixed wavelet bases and lacks adaptive processing of signal time-varying characteristics. Based on this, this paper adopts MI-driven adaptive wavelet base selection combined with GA-PSO hybrid optimization strategy, which can not only dynamically extract the most representative traveling wave features, but also realize parameter collaborative optimization at the global and local levels. It is a key breakthrough in the dual bottlenecks of signal adaptation and parameter optimization of current methods.

3. Improved WNN Cable Fault Location Model

A. WNN

WNN is a neural network model that combines wavelet transform with neural network. By using wavelet basis function as activation function, it can better extract the time-frequency characteristics of the signal and has strong localization characteristics [22]. Wavelet transform can effectively capture the instantaneous change information in the signal [23-25], while neural network uses its powerful nonlinear mapping ability for pattern recognition and learning. For WNN, wavelet transform generates multi-scale wavelet coefficients by performing multi-scale processing on the input signal. The processing formula of wavelet transform is shown in (1).

$$W(z,a,b)=\frac{1}{\sqrt{a}}\int_{-\infty}^{\infty} f(t)\beta\left(\frac{t-b}{a}\right)\mathrm{d}t \quad (1)$$

$f(t)$ represents the input signal, $\beta()$ represents the wavelet basis function, a represents the scaling factor, and b represents the translation factor.

In WNN, the input layer uses the input cable TW signal, and the hidden layer transforms the wavelet coefficients through a nonlinear activation function to simulate the relationship between the signal and the fault point. The output h_i of each hidden layer node is calculated by formula (2), and the formula expression is shown in formula (2).

$$h_i=\sigma\left(\sum_{j=1}^{n}\gamma_{ij}z_j+\delta_i\right) \quad (2)$$

γ_{ij} represents the weight from the input to the hidden layer node, z_j represents the input signal, and δ_i represents the bias term. σ represents the nonlinear activation function sigmoid.

In the output layer, the output is the location y of the cable fault point, and the calculation formula is shown in (3).

$$y=\sum_{i=1}^{m}\gamma_{oi}h_i+\delta_o \quad (3)$$

γ_{oi} represents the weight of the output layer, and δ_o represents the bias term of the output layer.

The improved WNN fault location model is shown in Figure 1. In Figure 1, the left side shows the improved steps, the adaptive wavelet basis selection based on MI and the GA-PSO optimization algorithm, the middle shows the structure of WNN, and the right side shows the output cable fault location result.

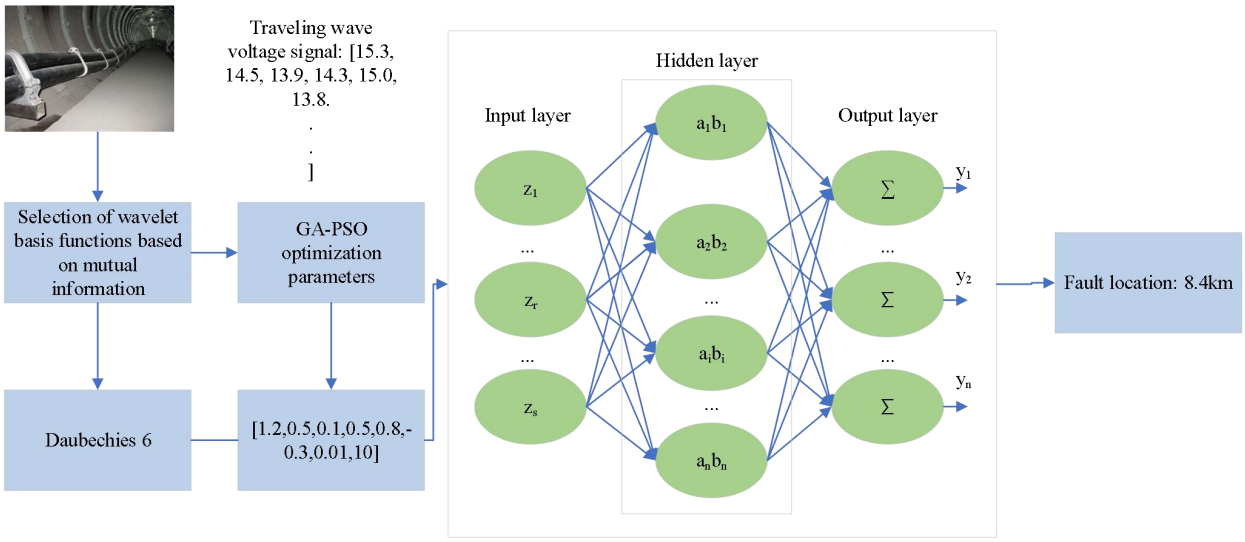

Figure 1. Improved WNN fault location model.

In Figure 1, after the cable TW signal is calculated through MI, the best wavelet basis is selected. Then the WNN improved by GA-PSO algorithm is used to locate the cable fault and output the fault distance from the starting point, which corresponds to 8.4km in the Figure 1.

The improved WNN fault location model in Figure 1 takes the cable TW signal as input, measures the correlation between each candidate wavelet basis and the fault signal characteristics through MI, and automatically selects the optimal wavelet basis to ensure efficient extraction of signal details. The selected wavelet basis is then applied to the hidden layer nodes of WNN, and GA is used to perform a global search for the scaling factor, translation factor, network weight, threshold, and number of hidden nodes to obtain the initial optimal parameters. Finally, the initial solution is used as the initial population, and PSO is introduced for local fine tuning to further improve the network fitting accuracy. The trained model directly gives the distance from the fault point to the starting point at the output layer, realizing end-to-end fault location from feature selection to parameter optimization.

B. Improvement of WNN

1) MI-Driven Adaptive Selection of Wavelet Basis

In the fault location of medium voltage cables, the characteristics of the signal are highly nonlinear and time-varying. Fixed wavelet bases are used in traditional WNN, which are difficult to adapt to real-time changes. This paper adopts a wavelet base adaptive selection method based on MI drive, which uses MI to measure the matching degree between different wavelet bases and signal characteristics, and automatically selects the optimal wavelet base that best suits the current signal characteristics.

MI is a statistic that measures the correlation between two random variables and is widely used in signal processing and feature selection [26,27]. This study uses MI to quantify the amount of information between different wavelet bases and the original fault signal, selects the wavelet base that is most relevant to the signal characteristics, and optimizes the feature extraction of the signal. For each pair of signal and wavelet coefficient, the calculation formula of MI $I(X,Y)$ is shown in (4).

$$I(X,Y)=\sum_{x\in X}\sum_{y\in Y}q(x,y)\log\left(\frac{q(x,y)}{q(x)q(y)}\right) \quad (4)$$

$q(x,y)$ represents the joint probability distribution of X and Y, $q(x)$ and $q(y)$ represent their respective marginal probability distributions. X represents the features extracted by the wavelet basis function, and Y represents the features of the original cable fault signal.

After calculating the MI value of all wavelet bases, the one with the largest MI value is selected as the optimal wavelet base of the current signal, and ζ_{op} is shown in formula (5).

$$\zeta_{op}=\underset{\zeta\in\hat{\zeta}}{\arg\max}\, I(X,Y) \quad (5)$$

Among them, ζ_{op} represents the wavelet basis that best matches the input signal, and $\hat{\zeta}$ represents the set of all candidate wavelet basis functions.

The MI comparison of different wavelet basis functions is shown in Table 1.

Table 1. MI comparison of different wavelet basis functions.

Wavelet basis function	MI value	Wavelet basis function	MI value
Haar wavelet	0.782	Daubechies 3	0.846
Coiflet 3	0.9	Daubechies 4	0.915
Symlet 4	0.875	Daubechies 5	0.935
Morlet wavelet	0.795	Daubechies 6	0.965
Mexican hat	0.77	Daubechies 7	0.955

In Table 1, according to the MI comparison of different wavelet basis functions, the one with the largest MI value is Daubechies 6, which is the final wavelet basis function of this paper.

2) Optimization of GA-PSO Algorithm

(1) GA algorithm

In WNN, this paper introduces GA to optimize the global search process of the network to avoid it from falling into the local optimal solution [28,29]. GA simulates the process of natural selection and uses the fitness function to guide the search process to obtain the optimal solution.

In GA, it now initializes a population, and each individual represents a set of possible solutions [30]. The chromosome of an individual consists of a series of real-valued numbers, and each position represents a parameter in the network. The gene encoding of each individual in the population is shown in equation (6).

$$P_i = \{p_{i1}, p_{i2}, \cdots, p_{in}\} \quad (6)$$

p_{i1} to p_{in} represent the hyperparameters of WNN, which are the scaling factor, translation factor, network connection weight, threshold, and number of hidden nodes, respectively. P_i represents the i-th individual.

In the optimization process of WNN, the fitness function mainly measures the positioning accuracy of the network. The fitness function $F(P_i)$ is shown in formula (7).

$$F(P_i) = \frac{1}{1 + \left| y_{\mathrm{pr}} + y_{\mathrm{ac}} \right|} \quad (7)$$

y_{pr} represents the predicted fault location, and y_{ac} represents the actual fault location.

The selection operation selects individuals from the current population according to fitness as the parents of the next generation. This paper adopts the roulette selection method for parent selection. The probability $Q_{\mathrm{se}}(P_i)$ of an individual being selected is shown in formula (8).

$$Q_{\mathrm{se}}(P_i) = \frac{F(P_i)}{\sum_{j=1}^{N} F(P_j)} \quad (8)$$

This paper simulates the gene recombination process through crossover operation, generating offspring by exchanging gene fragments between two parent individuals. P_a and P_b of the two parent individuals are shown in formulas (9) and (10).

$$P_a = \{p_{a1}, p_{a2}, \cdots, p_{an}\} \quad (9)$$

$$P_b = \{p_{b1}, p_{b2}, \cdots, p_{bn}\} \quad (10)$$

B_1 and B_2 after single-point crossover are shown in equations (11) and (12).

$$B_1 = \{p_{a1}, p_{a2}, \cdots, p_{ak}, p_{b(k+1)}, p_{b(k+2)}, \cdots, p_{bn}\} \quad (11)$$

$$B_2 = \{p_{b1}, p_{b2}, \cdots, p_{bk}, p_{a(k+1)}, p_{a(k+2)}, \cdots, p_{an}\} \quad (12)$$

k represents the crossover point, and B_1 and B_2 represent the offspring individuals obtained after the crossover operation.

In the mutation operation, randomness is introduced to help the algorithm escape from the local optimum and ensure the diversity of the population. Mutation randomly changes the value of a gene in an individual, and the new gene value p'_{ij} is shown in formula (13).

$$p'_{ij} = p_{ij} + \eta \cdot ra(0,1) \quad (13)$$

η represents the variation amplitude, p'_{ij} represents the new gene value. $ra(0,1)$ represents a random number between 0 and 1.

The study generated a new population through selection, crossover and mutation operations. The next generation of population can enter a new evolutionary cycle, repeating operations such as selection, crossover, and mutation until the predetermined number of iterations is reached or the fitness reaches the set threshold. When any of the termination conditions is met, the algorithm ends, and the individual with the highest fitness is finally selected as the optimal solution.

(2) PSO algorithm

In the optimization process of WNN, GA is mainly used for global search to obtain a more reasonable preliminary solution, while PSO fine-tunes the preliminary solution

through local search. PSO is an optimization algorithm based on swarm intelligence, which simulates the behavior of particles flying in the search space to find the optimal solution of the problem [31,32].

In the PSO algorithm, each particle represents a potential solution, and the position of the particle corresponds to a set of solutions for the network parameters [33]. At initialization, each position of the particle is assigned to the preliminary solution obtained by GA optimization. The position update C_i^{d+1} of each particle is shown in formula (14).

$$C_i^{d+1} = C_i^d + V_i^{d+1} \quad (14)$$

C_i^d represents the position information of the particle in the dth generation, V_i^{d+1} represents the velocity information of the particle in the $d+1$ th generation, and C_i^{d+1} represents the position information of the particle in the $d+1$ th generation.

The PSO algorithm adjusts the velocity of each particle through information transmission between particles, so that it can effectively explore and utilize the solution space. The particle velocity update V_i^{d+1} is shown in formula (15).

$$V_i^{d+1} = \iota \cdot V_i^d + \lambda_1 \cdot \xi_1 \cdot \left(po_i^{\text{best}} - C_i^d \right) + \lambda_2 \cdot \xi_2 \cdot \left(gr_i^{\text{best}} - C_i^d \right) \quad (15)$$

ι represents the inertia weight, λ_1 and λ_2 represent the learning factors, and ξ_1 and ξ_2 represent random numbers. po_i^{best} represents the best position of the particle in history, and gr_i^{best} is the best position among all particles.

In the fitness function design, similar to the fitness function in the GA algorithm, the fitness function of the PSO algorithm is used to measure the quality of the particle solution. The fitness function $F\left(C_i\right)$ is shown in formula (16).

$$F\left(C_i\right) = \frac{1}{1 + \left| y_{\text{pr}}\left(C_i\right) + y_{\text{ac}} \right|} \quad (16)$$

$y_{\text{pr}}\left(C_i\right)$ represents the network prediction output based on the current parameter settings of the particle.

In the PSO algorithm, each particle maintains an individual best position po_i^{best}, which corresponds to the best solution encountered by the particle during the search process. The global best position gr_i^{best} corresponds to the solution with the best fitness among all particles.

At each iteration, if the current fitness of the particle is better than the individual best fitness, the individual best position is updated. If the current fitness is better than the global best fitness, the global best position is updated. The update rules of po_i^{best} and gr_i^{best} are shown in equations (17) and (18).

$$po_i^{\text{best}} = C_i^d \qquad F\left(C_i^d\right) > F\left(po_i^{\text{best}}\right) \quad (17)$$

$$gr_i^{\text{best}} = C_i^d \qquad F\left(C_i^d\right) > F\left(gr_i^{\text{best}}\right) \quad (18)$$

Based on the preliminary solution obtained by GA, the PSO algorithm further optimizes the hyperparameters of WNN. In the fault point location of medium-voltage cables, PSO further improves the prediction accuracy of the network by fine-tuning the network parameters. The particle swarm performs multiple iterations in the local space and gradually converges to a better solution, reducing the influence of the local optimal solution.

The termination condition of the PSO algorithm is to reach the maximum number of iterations or the fitness function reaches a predetermined threshold. When any of the termination conditions is met, the algorithm ends and outputs the current global optimal solution.

After the above steps, the output parameters of the experiment are as follows: the scaling factor is 1.2, the translation factor is 0.5, the network connection weight is [0.1, 0.5, 0.8, -0.3], the threshold is 0.01, and the number of hidden nodes is 10.

The interactive structure diagram of the GA-PSO algorithm is shown in Figure 2. In Figure 2, the interactive steps are as follows:

1) Initialize the population and particles, and calculate the fitness function under GA optimization.

2) Perform selection, crossover and mutation operations, and output a new population.

3) Send the new population to PSO optimization, recalculate the fitness function, and update the global position and historical optimal position of the particles in turn.

4) Update the particle speed and particle position.

5) Output the optimal network parameters.

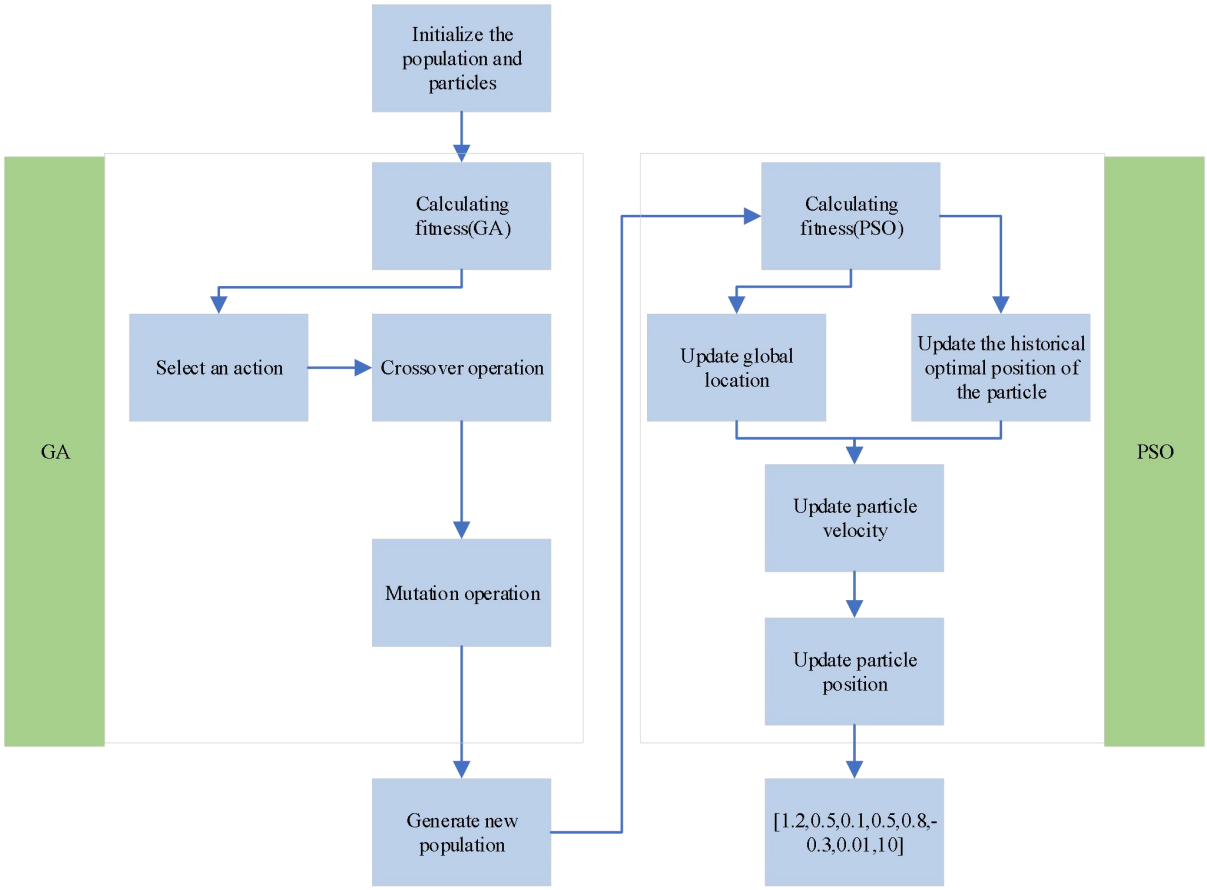

Figure 2. Interaction structure diagram of GA-PSO algorithm.

In Figure 2, the GA-PSO algorithm is different from the traditional connection method of extracting some functions. This paper adopts a serial connection method for mixing, using the execution result of the GA part as the initial matrix of the PSO part.

Figure 2 shows the serial interaction structure of GA-PSO hybrid optimization in WNN parameter tuning. The GA part initializes a population consisting of network hyperparameters, and through selection, crossover, mutation operations and fitness evaluation, it repeatedly evolves to produce a set of excellent candidate solutions obtained by global search. Then the PSO part receives the preliminary optimal particle group output by the GA as the initial position, and uses the information exchange mechanism between particles and the speed-position update formula to further iterate and optimize in the local area. In each iteration, PSO dynamically adjusts the particle speed and position according to the individual best and global best information to more finely approximate the optimal parameter combination. When the maximum iteration or fitness threshold is reached, the final global optimal parameters are output to complete the joint optimization of WNN. Through this serial design, this paper not only ensures the global exploration ability of the algorithm, but also takes into account the convergence speed and local fine adjustment, effectively avoiding the problem of a single optimizer falling into local optimality or slow convergence.

C. Training and Optimization of Network Model

1) Loss Function Design

This study uses MSE as the loss function to evaluate the gap between the network predicted location and the actual fault location. The loss function $L(\theta)$ is shown in formula (19).

$$L(\theta)=\frac{1}{N}\sum_{i=1}^{N}\left(y_{\mathrm{pr}}(i)-y_{tr}(i)\right)^{2} \quad (19)$$

θ represents the parameter set of the network.

In order to further enhance the network's adaptability to local signal features, this paper introduces the L2 regularization term in the loss function to prevent the network from overfitting. The L2 regularization expression $L_{\mathrm{re}}(\theta)$ is shown in formula (20).

$$L_{\mathrm{re}}(\theta)=o\sum_{j=1}^{M}\theta_{j}^{2} \quad (20)$$

o represents the regularization parameter.

The final loss function expression L_{to} is shown in formula (21).

$$L_{\text{to}} = L(\theta) + L_{\text{re}}(\theta) \quad (21)$$

L_{to} represents the total loss function.

2) Model Optimization

In actual fine-grained optimization, GA and PSO are mainly used for global optimization and local refinement, which are very useful when exploring parameter space. This paper introduces Adam to further optimize the network training process [34,35], and the expression of parameter update is shown in (22).

$$\vartheta_t = \vartheta_{t-1} - \frac{\varpi \hat{\rho}_t}{\sqrt{\hat{\varrho}_t} + \varsigma} \quad (22)$$

ϖ represents the learning rate, $\hat{\rho}_t$ and $\hat{\varrho}_t$ represent the corrected estimates.

The hyperparameters of the three algorithms WNN, GA and PSO in the experiment are shown in Table 2.

Table 2. Hyperparameters of the three algorithms WNN, GA and PSO.

WNN		GA		PSO	
Parameters	Value	Parameters	Value	Parameters	Value
Learning rate	0.001	Population size	50	Number of particles	30
Regularization parameter	0.01	Crossover rate	0.8	Position update coefficient	0.5
Activation function	Sigmoid	Mutation rate	0.1	Individual learning factor	1.5
Number of input layer nodes	20	Maximum number of iterations	100	Group learning factor	1.5
Number of output layer nodes	1	Selection method	Roulette selection	Maximum speed	2

4. Experimental Design For Locating Fault Points of Medium-Voltage Cables

A. Experimental Data

The experimental data is generated by simulating the actual operating environment of medium-voltage cables and signal reflections under different fault types and fault point locations. Fault types include short circuit, open circuit, ground fault, etc. The power supply voltage is 35kv, the frequency is 50Hz, and the cable lengths include 100km, 200km, 300km, 400km, 500km, 600km, 700km, and 800km. The fault start and end time is set to 0.03 to 0.035s, the simulation time is set to 0.1s, and the signal sampling frequency is 10kHz.

This paper takes 100km as an example, and sets the cable fault at a distance of 2km, with an interval of 2-80km. The collected data are the modulus maximum points of the fault voltage TW. A total of 40 sets of data were collected as the training set for the 100km cable length at this time, and 8 sets of data from 5km to 75km were used as the test set, corresponding to 5km, 15km, 25km, 35km, 45km, 55km, 65km, and 75km positions. The verification of the remaining seven sets of fault distances is the same as above, and the cable setting distances are consistent. When the cable length is 200km, the fault interval is 102km to 180km, the distance is 2km, and the data from 105km to 175km is used as the test set. The corresponding fault points are 105km, 115km, 125km, 135km, 145km, 155km, 165km, and 175km.

B. Data Preprocessing

The amplitude of the cable fault signal can vary greatly in different tests. In order to ensure the uniformity of the training data and the stability of the network training, this paper uses Min-Max normalization to normalize the signal. The formula is shown in (23).

$$Z' = \frac{Z - Z_{\min}}{Z_{\max} - Z_{\min}} \quad (23)$$

Among them, Z' represents the normalized signal, $Z_{\min}$ and $Z_{\max}$ represent the minimum and maximum values of the signal respectively.

C. Evaluation Indicators

In order to prove the advantages of the improved GA-PSO-WNN method in locating medium-voltage cable fault points, this paper uses indicators such as number of iterations, convergence time, MAE, RMSE, MAPE, error value, and error under noise and different cable lengths to fully reflect the performance of the algorithm in practical applications.

The number of iterations and convergence time can intuitively reflect the convergence speed of the method. Fewer iterations and shorter convergence time indicate that the algorithm is more efficient in finding the optimal solution and can quickly find satisfactory results. MAE, RMSE, and MAPE are commonly used indicators for evaluating positioning accuracy. They can quantify the error between the positioning result and the actual fault point, especially in complex environments. They can better verify the ability of the improved algorithm to reduce positioning errors. Through these indicators, the experiment can comprehensively evaluate whether the GA-PSO-WNN method can effectively improve positioning accuracy, optimize global search capabilities, and increase convergence speed, especially in practical application scenarios such as different cable lengths and noise interference.

The error value and the error under noise and different cable lengths further verify the robustness and stability of the algorithm in a changing environment. The

experiment tests the improved method under different cable lengths and noise intensities to reflect its adaptability and practical application effect in a complex environment.

The calculation formula of MAE is shown in (24):

$$MAE = \frac{1}{N}\sum_{i=1}^{N}\left|y_{\mathrm{pr}}(i) - y_{\mathrm{tr}}(i)\right| \quad (24)$$

The calculation formula of $MAPE$ (Mean Absolute Percentage Error) is shown in (25):

$$MAPE = \frac{1}{N}\sum_{i=1}^{N}\frac{\left|y_{\mathrm{pr}}(i) - y_{\mathrm{tr}}(i)\right|}{y_{\mathrm{tr}}(i)} * 100\% \quad (25)$$

The calculation formula of $RMSE$ is shown in (26):

$$RMSE = \sqrt{\frac{1}{N}\sum_{i=1}^{N}\left(y_{\mathrm{pr}}(i) - y_{\mathrm{tr}}(i)\right)^2} \quad (26)$$

D. Experimental Design

To verify the effectiveness and robustness of the medium voltage cable fault location method based on the improved WNN, this paper designed multiple experiments covering scenarios with different cable lengths and different noise interference intensities. The main goal of the experiment is to evaluate the positioning accuracy, real-time performance, and robustness of the model in a variable actual environment.

The experiment was first conducted under different cable lengths to simulate the impact of different cable operating environments on fault location accuracy. The selection of cable lengths took into account various common scenarios in actual power systems, including short, medium and long distance cables, which are 100km, 200km, 300km, 400km, 500km, 600km, 700km and 800km respectively. The experiment also adds Gaussian noise of different intensities to interfere with the fault signal, compares the difference between the positioning accuracy under different noise interference and the noise-free state, and analyzes the stability of the system. The noise ranges from 5dB to 40dB. In the experiment, the experimental method is GA-PSO-WNN (adaptive wavelet basis), and the control methods include TW method, impedance method, BP (back propagation), CSA-WNN, GA-WNN, PSO-WNN, WNN, SSA-WNN (Sparrow Search Algorithm-Wavelet Neural Network).

5. Display of Medium Voltage Cable Fault Location Results

A. Cable Fault Location Distance Difference Diagram

The experiment takes the case of a cable length of 100km as an example, conducts simulation experiments on different methods, and statistically analyzes the cable fault location results on the test set, as shown in Figure 3. In Figure 3, the location errors of the fault location at 5km, 15km, 25km, 35km, 45km, 55km, 65km, and 75km are displayed. The horizontal axis represents the method name, and the vertical axis represents the distance difference.

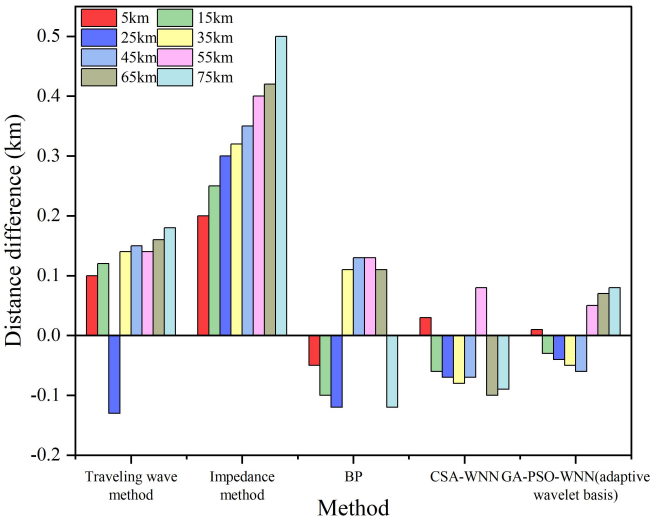

Figure 3. Positioning results.

In Figure 3, GA-PSO-WNN (adaptive wavelet basis) shows the smallest error at each test point, with an error range of -0.06km to 0.08km, significantly better than other methods, with the error at the 5km fault point being only 0.01km. The error of CSA-WNN is slightly larger, ranging from -0.10km to 0.08km, indicating that the introduction of swarm intelligence optimization algorithm has improved the positioning accuracy to a certain extent, but it is still not as good as the joint optimization of GA and PSO. The error of BP neural network fluctuates greatly, with an error of -0.1km at 15km and 0.13km at 55km, showing a certain degree of prediction instability. Traditional methods such as the TW method and the impedance method have larger errors, ranging from -0.13km to 0.18km and 0.2km to 0.5km respectively, and have poor adaptability to complex fault characteristics.

GA-PSO-WNN improves the ability to extract instantaneous high-frequency features by introducing an adaptive wavelet basis for fine signal modeling. At the same time, it combines the global search of GA with the local refinement optimization of PSO to effectively adjust the scaling factor, translation factor and network parameters to achieve more accurate fault location. Although CSA-WNN has certain optimization capabilities, it has not achieved two-stage evolution and has limited optimization accuracy. BP only relies on gradient descent and is prone to fall into local optimality, resulting in a significant decrease in prediction accuracy at points where the fault location changes sharply, such as 65km and 75km. The main reason for the increase in errors is that the TW method and the impedance method rely too much on a single characteristic parameter and ignore the complex changes in the reflected waveform.

B. *Convergence Curve Analysis*

The convergence curves of different methods tested under a cable length of 100 km are shown in Figure 4. In Figure 4, the horizontal axis represents the number of iterations and the vertical axis represents the fitness value. The higher the fitness value, the better the model fits the training data, the smaller the positioning error, and the better the overall performance. The improvement of the fitness value means that the algorithm has more advantages in global search and local fine-tuning, and can optimize network parameters more accurately, improving the accuracy and robustness of medium-voltage cable fault point positioning.

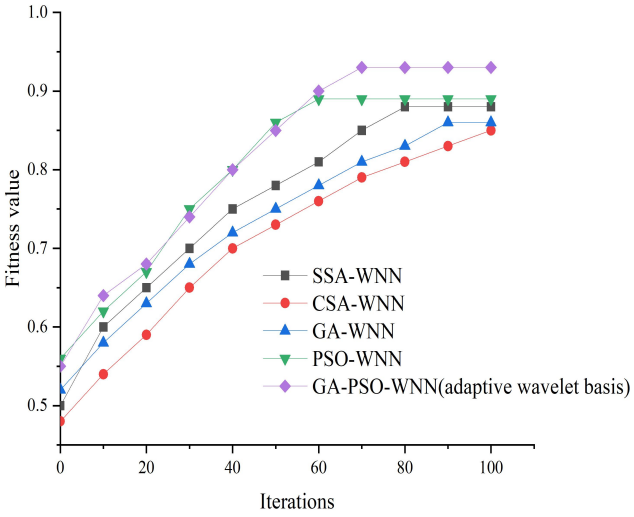

Figure 4. Convergence curves of different methods tested under 100km cable length.

In Figure 4, as a whole, as the number of iterations increases, the fitness value gradually increases and the convergence tends to be stable. PSO-WNN has the fastest convergence speed, reaching a convergence state after 60 iterations, and the fitness value reaches 0.89. The GA-PSO-WNN (adaptive wavelet basis) in this paper converges faster, reaching the convergence level after 70 iterations, and the fitness is the largest, reaching 0.93. The convergence speed of GA-WNN is slower, reaching the convergence state after 90 iterations, and the fitness is average, reaching 0.86. For CSA-WNN, its fitness value is the lowest, only 0.85 after 100 iterations, and it has not reached the convergence state. SSA-WNN reaches convergence after 80 iterations, and the fitness value reaches 0.88. In summary, this paper introduces adaptive wavelet basis, GA, and PSO to achieve better convergence speed and improve positioning accuracy.

C. *Fault Point Positioning Results under Different Cable Lengths and Different Noise Interference*

In order to explore the robustness of the improved WNN in this paper, the fault location error is tested under different cable lengths and different noises, and the results are shown in Figure 5. In Figure 5 (a), the horizontal axis represents the cable length, in Figure 5 (b), the horizontal axis represents the noise intensity, and the vertical axis represents the error value, specifically *MAE*, *RMSE*, and *MAPE*. *MAE* measures the average positioning error. The smaller the value, the higher the overall accuracy. *RMSE* reflects the stability and discreteness of the error. The smaller the value, the more concentrated the error. *MAPE* is used to measure the relative error. The smaller the value, the higher the relative accuracy of the model.

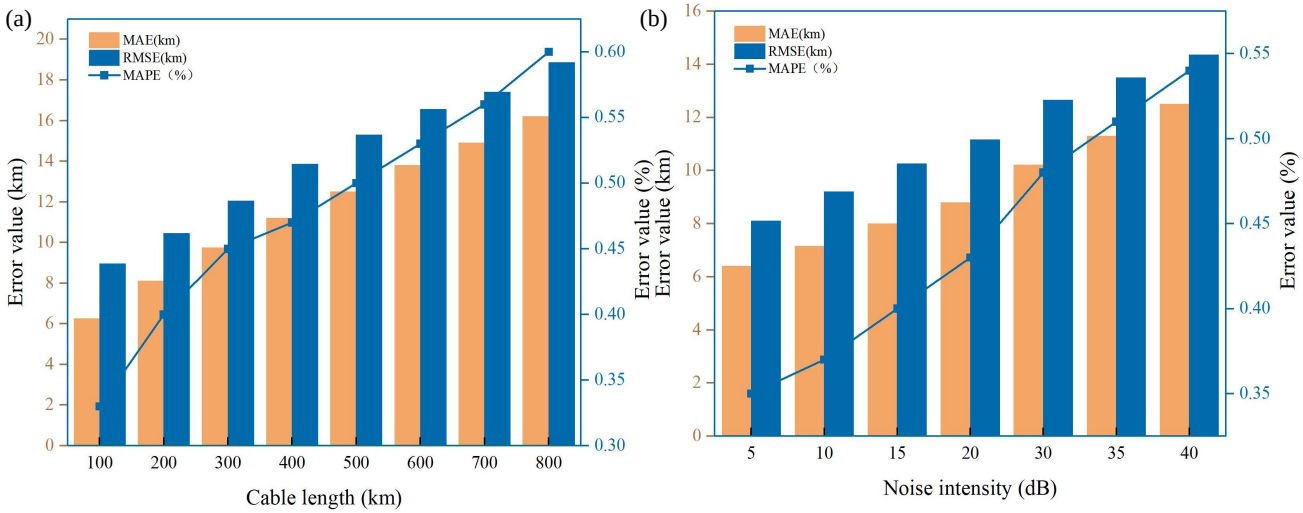

Figure 5. Fault location results under different cable lengths and different noise interferences. Figure 5 (a) Fault location results under different cable lengths; Figure 5 (b) Fault location results under different noises.

In the test results under different cable lengths in Figure 5 (a), both *MAE* and *RMSE* increase with the increase of cable length, indicating that the longer the cable, the more significant the attenuation and interference of the fault signal, resulting in a decrease in positioning accuracy. When the cable length is 100 km, the *MAE* is 6.25 km and the *RMSE* is 8.95 km. When the cable length increases to 800 km, the *MAE* increases to 16.2 km and the *RMSE* increases to 18.85 km. It can be seen that the distortion of the time domain characteristics caused by attenuation, dispersion and reflection during the propagation of TWs reduces the

ability of WNN to extract distant fault points. Looking at the *MAPE* under different cable lengths, the *MAPE* is 0.33% at 100 km, and rises to 0.60% at 800 km, nearly doubling. The longer the cable, the more complex the signal propagation path, and the more difficult it is to completely filter out the superimposed interference and background noise, which poses a challenge to the reliability of fault feature extraction.

Under different noise intensity conditions in Figure 5 (b), *MAE* and *RMSE* also show a significant upward trend. When the noise intensity is 5dB, the *MAE* and *RMSE* are 6.4km and 8.1km respectively; when the noise intensity is increased to 40dB, the two indicators reach 12.5km and 14.35km respectively. This phenomenon shows that although the model has a certain degree of noise resistance, the recognition accuracy of key feature points decreases under high-intensity noise interference, resulting in an increase in the overall positioning error.

As for the change of *MAPE* under noise interference, it gradually increases from 0.35% at 5dB to 0.54% at 40dB, showing a stable increasing trend. The noise superposition interferes with the characteristic structure of the original TW signal and increases the non-stationarity of the input data. Even if the adaptive wavelet basis has a good decomposition ability for high-frequency components, it cannot completely eliminate the pseudo-features, which affects the accuracy of the neural network's judgment of the real fault point. In summary, the error of the improved WNN method in this paper is generally at a low level under different cable lengths, and it has a certain anti-interference ability for different noise intensities.

The reason for the difference in errors under different cable lengths and noise intensities is mainly due to the changes in physical properties and the increase in noise interference experienced by the TW signal during transmission. As the cable length increases, the TW signal needs to propagate over a longer distance, which can cause more obvious attenuation, dispersion effect and multiple reflection interference, resulting in time domain broadening, amplitude reduction and waveform distortion of the original signal characteristics. This makes it difficult for the modulus maximum feature points extracted by the adaptive wavelet basis to accurately reflect the actual fault location, thus affecting the training and prediction accuracy of the WNN. When the noise interference is enhanced, especially when the noise intensity is greater than or equal to 30dB, a large number of high-frequency pseudo features can be mixed in the TW signal, which increases the uncertainty in the feature extraction process. This paper introduces the GA-PSO optimization algorithm to jointly optimize the WNN network parameters, using the global search capability of GA to avoid falling into the local optimum, and using the fast local search characteristics of PSO to accelerate the convergence speed, thereby improving the generalization ability and stability of the model. At the same time, combined with the MI-driven adaptive wavelet basis selection mechanism, feature extraction is more targeted and robust, and feature information reflecting the real fault location can still be effectively extracted in the face of long-distance transmission and high-intensity noise interference. Experimental results show that the improved WNN method in this paper shows good robustness and high positioning accuracy under different working conditions, verifying the effectiveness and practicality of the GA-PSO optimization strategy and adaptive wavelet basis collaborative mechanism in the task of locating medium-voltage cable fault points.

D. Real-time Performance of Fault Location of Different Methods

The real-time performance results of fault location of different methods are shown in Figure 6. In Figure 6, the horizontal axis represents the method name, and the vertical axis represents the time, specifically the fault location time, processing delay time, and response time.

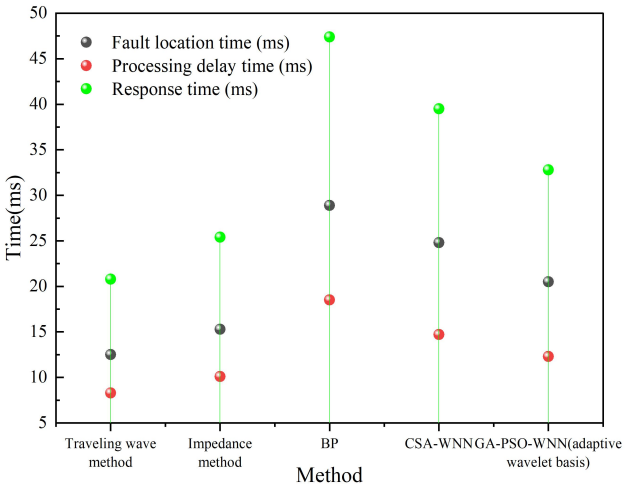

Figure 6. Real-time results of fault location of different methods.

In Figure 6, the traditional methods of TW method and impedance method have significant response speed advantages. The fault location time of TW method is 12.5ms, the processing delay time is 8.3ms, and the overall delay is the shortest. The fault location time and processing delay time of the impedance method are 15.3ms and 10.1ms respectively. The location time of the BP method is 28.9ms, and the processing delay is 18.5ms, which is higher than the traditional algorithm. CSA-WNN and GA-PSO-WNN (adaptive wavelet basis) have higher computational efficiency with the support of optimization strategy, with location time of 24.8ms and 20.5ms respectively, and processing delay time of 14.7ms and 12.3ms respectively.

In terms of response time, GA-PSO-WNN (adaptive wavelet basis) outperforms all neural network methods, with a response time of 32.8ms, while CSA-WNN reaches 39.5ms and BP reaches 47.4ms. The TW method and impedance method maintain the lowest response time at 20.8ms and 25.4ms respectively, but the positioning accuracy is much lower than GA-PSO-WNN

(adaptive wavelet basis). In summary, while maintaining a relatively fast response speed, GA-PSO-WNN (adaptive wavelet basis) achieves a better balance in terms of accuracy and stability, reflecting its dual guarantee of real-time and accuracy in medium-voltage cable fault location.

In the comparison of the real-time performance of fault location of different methods, the differences presented are mainly closely related to the complexity of the algorithm structure, the feature extraction mechanism, and the computational efficiency of the optimization strategy. Traditional methods such as the TW method and the impedance method rely on fixed formulas and threshold judgments. The algorithm logic is simple, the amount of calculation is small, and it has an extremely fast response speed. It is suitable for scenarios with extremely high real-time requirements, but its robustness and positioning accuracy are insufficient in complex environments, and it is difficult to adapt to situations where the signal has obvious nonlinear characteristics. Neural network methods such as BP, CSA-WNN, and GA-PSO-WNN can effectively capture complex signal characteristics and improve positioning accuracy due to the introduction of nonlinear modeling capabilities, but it also brings about the problem of increased model calculation and longer reasoning time. The BP method has a slow convergence speed and inefficient reasoning process due to the lack of a global optimization mechanism, and performs worst in positioning time and response time. Although CSA-WNN introduces swarm intelligence optimization to improve accuracy, its algorithm has a large search space and weak local convergence ability, which also causes a certain response delay.

The GA-PSO-WNN (adaptive wavelet basis) used in this paper is more efficient in network parameter initialization and fine-tuning by integrating the global search of GA and the local optimization mechanism of PSO, and reduces redundant features with the wavelet basis selection mechanism driven by MI. This enables the neural network to reduce the burden of feature extraction and model calculation while maintaining the accuracy advantage, significantly improving the reasoning efficiency and overall response time. The GA-PSO-WNN (adaptive wavelet basis) method achieves a better trade-off between real-time and accuracy, demonstrating its engineering adaptability and application prospects in complex cable fault scenarios.

E. Ablation Experiment

This paper introduces GA and PSO, and the adaptive wavelet basis is used to improve WNN. In order to explore their respective effects on positioning accuracy and convergence speed, this paper adopts ablation experiments. The specific experimental process is as follows:

(1) Complete model benchmark test: GA-PSO-WNN (adaptive wavelet basis), the model contains all three improved modules: GA, PSO and adaptive wavelet basis.

(2) Module 1 adaptive wavelet basis can be removed, and only the WNN optimized by GA and PSO (GA-PSO-WNN) can be retained to verify the improvement effect of adaptive wavelet basis in signal feature extraction and model training.

(3) Module 2 PSO algorithm can be removed, GA can be retained, and a GA-WNN structure can be formed to evaluate the role of PSO in optimizing convergence speed and parameter tuning.

(4) Module 3 GA algorithm can be removed, PSO can be retained, and a PSO-WNN structure can be formed to analyze the contribution of GA in improving model diversity and global search capabilities.

(5) GA and PSO can be removed and the most basic WNN structure can be used. This structure is used as a control group to reflect the comprehensive impact of the three improvements on the model performance.

Now the experiment is carried out in an environment with a cable length of 100 km. The results are shown in Table 3.

Table 3. Ablation experiment results.

Method	*MAE* (km)	*MAPE* (%)	*RMSE* (km)	Convergence speed (epochs)
GA-PSO-WNN(adaptive wavelet basis)	6.25	0.33	8.95	70
GA-PSO-WNN	6.85	0.35	9.3	76
GA-WNN	7.5	0.38	10.1	90
PSO-WNN	7.95	0.41	10.75	60
WNN	8.2	0.43	11.2	118

In Table 3, it can be seen that GA-PSO-WNN (adaptive wavelet basis) has the lowest fault location error, with *MAE* of 6.25km, RMSE of 8.95km, and *MAPE* of 0.33%. When the adaptive wavelet basis is removed and only GA-PSO-WNN is used, the *MAE* is 6.85km, *RMSE* is 9.3km, and *MAPE* is 0.35%. It can be seen that the introduction of the adaptive wavelet basis improves the performance of the network to a certain extent, optimizes the feature extraction of the signal and the learning ability of the network.

When the PSO algorithm is removed, the *MAE* of GA-WNN is only 7.5km and the RMSE is only 10.1km, and the positioning error is significantly improved. After removing GA, the MAE of PSO-WNN is 7.95km and the *RMSE* is 10.75km. This shows that after removing GA,

the performance of the model decreases more significantly than after removing PSO, which proves the importance of GA in optimizing population diversity.

When GA, PSO and adaptive wavelet base are completely removed and traditional WNN is used, the positioning error increases further, with *MAE* of 8.2km, RMSE of 11.2km and MAPE of 0.43%. It shows that the optimization strategy of GA and PSO and the introduction of adaptive wavelet basis have significantly improved the fault location performance of WNN and effectively avoided falling into the local optimal solution. Compared with the single GA and PSO, the global search capability is improved, the adaptability and robustness of the model are improved, and the location error is reduced, which proves the important role of these modules in improving accuracy.

For the convergence speed in Table 3, the convergence speed of the GA-PSO-WNN (adaptive wavelet basis) model is 70 iterations, which performs relatively well. It can be seen that the synergistic effect of the three improvement methods not only improves the positioning accuracy, but also significantly accelerates the convergence efficiency of training. The enhancement of feature extraction by adaptive wavelet basis helps the model to quickly capture key information and accelerate the network learning process. The collaborative optimization of GA and PSO effectively adjusts the weight and threshold parameters and accelerates the search process. When the adaptive wavelet basis is removed and only GA and PSO are retained, the number of iterations required for model convergence increases to 76 times, indicating that although the global optimization capability still exists, the lack of the wavelet basis's local fine expression ability of the signal makes the model training process slightly slow. Further analysis shows that the convergence speed after removing PSO alone is 90 times, which is slow. The PSO algorithm itself has a strong local search capability and can quickly approach the optimal area in the early stage of training. Removing it can result in an inefficient search path and a prolonged convergence process. The convergence speed of removing GA alone is 60 times, which is faster than GA-WNN. Although the accuracy has decreased, PSO provides a faster local search capability in the initial optimization process, and the training converges faster. However, this rapid convergence is often accompanied by the risk of falling into local optimality, resulting in a decrease in overall performance. The basic WNN structure has the slowest convergence speed, which is 118 iterations. It can be seen that the training process of the neural network without any optimization means is relatively slow when facing complex signals, and it is difficult to efficiently find a better solution.

In summary, different modules have different focuses on the impact of convergence speed. PSO is more conducive to rapid convergence in the early stage, GA focuses more on global search and parameter diversity, and adaptive wavelet basis improves feature extraction efficiency and training stability. The combination of the three in this paper can significantly shorten the model training cycle while maintaining accuracy improvement.

F. Power System Stability Analysis

In order to verify the voltage and current stability of the power system fault recovery process, an experiment is designed to simulate the recovery process of the power system after a fault occurs, and the system recovery capability after the cable fault occurs is analyzed according to different methods such as TW method, impedance method, BP, CSA-WNN, WNN, and GA-PSO-WNN (adaptive wavelet basis). In the experiment, an instantaneous short-circuit fault is artificially set in the system to simulate the instantaneous fluctuation of voltage and current. The fluctuation curves of voltage and current in the process from fault occurrence to recovery are shown in Figure 7. In Figure 7 (a), the horizontal axis represents time and the vertical axis represents voltage. In Figure 7 (b), the horizontal axis represents time and the vertical axis represents current.

In Figure 7 (a), it can be seen that when the fault occurs, the voltage fluctuation has obvious fluctuations, and the voltage fluctuation gradually decreases during the recovery process. In the TW method and impedance method, the voltage fluctuation is large, especially for a period of time after the fault, and the recovery time is long, about 13.6s and 15.3s respectively. The recovery effect of the BP, CSA-WNN, WNN and GA-PSO-WNN (adaptive wavelet basis) methods is better, the voltage fluctuation is reduced quickly, and the recovery process is smoother. The GA-PSO-WNN (adaptive wavelet basis) method has the smallest voltage fluctuation after recovery, which only takes about 6.2s. It shows a strong recovery ability, which is related to the optimization characteristics of its adaptive wavelet basis.

In Figure 7(b), the current fluctuations of all methods after the fault occurred are also large, and the fluctuations gradually decrease after recovery. The current fluctuations of the TW method and the impedance method are more severe, especially in the early stage after the fault occurs, and the current recovery is slow. The current recovery of the BP, CSA-WNN, WNN and GA-PSO-WNN (adaptive wavelet basis) methods is relatively rapid, especially the GA-PSO-WNN (adaptive wavelet basis) method, the current fluctuations recover to a near normal state in a relatively short time. GA-PSO-WNN (adaptive wavelet basis) has the best current recovery performance because it combines GA and PSO and has high efficiency in fault location and optimization of recovery strategy.

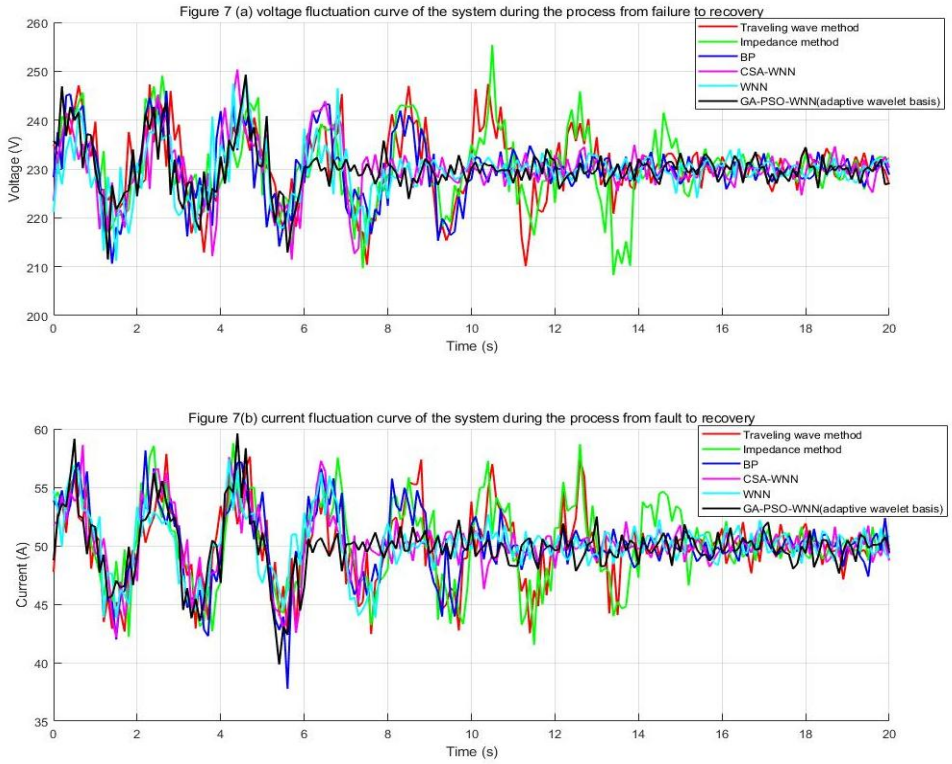

Figure 7. Voltage and current fluctuation curve of the system during the process from fault to recovery. Figure 7 (a) Voltage fluctuation curve of the system during the process from fault to recovery; Figure 7 (b) Current fluctuation curve of the system during the process from fault to recovery.

From the perspective of voltage fluctuation recovery, the differences in fault location accuracy and response strategy among different methods are the main reasons for the different recovery effects. Traditional TW method and impedance method rely on the propagation characteristics of fault reflection wave or line parameter calculation, which are sensitive to noise and system structure changes, easily causing error accumulation, prolonging positioning and recovery time, and resulting in long duration of voltage fluctuation. BP neural network and WNN methods have advantages in learning the nonlinear dynamic characteristics of the system, especially CSA-WNN and GA-PSO-WNN methods combined with intelligent optimization algorithms, which can achieve global optimization of network weights and wavelet basis functions, and improve the model's fitting and generalization capabilities. After fault location, the recovery process can be started faster, and voltage fluctuations decay quickly.

In the process of current fluctuation recovery, the algorithm's response speed to system disturbances and its adaptability to non-stationary signals become key factors. The TW method and impedance method need to rely on multi-point feature judgment and complex model matching processes after fault identification. The response speed is relatively lagging, and the current fluctuation lasts for a long time. Intelligent algorithms such as BP and WNN can quickly capture the characteristics of current mutations, extract effective fault modes, and accelerate the triggering of system control strategies. The GA-PSO-WNN method effectively avoids falling into local optimality by introducing GA and PSO mechanisms, enhances the ability to handle complex disturbances, and quickly restores the current to a steady state. This multi-agent collaborative optimization method improves the overall response efficiency of the system, which is the main reason for its optimal performance in current recovery.

G. System Recovery Time and Fault Downtime of Different Methods, Load Recovery Efficiency

In order to comprehensively evaluate the comprehensive performance of various methods in actual cable fault handling, this paper introduces the load recovery efficiency index, which is used together with the system recovery time and fault downtime as a comprehensive evaluation standard. The system recovery time refers to the time from the occurrence of the fault to the restoration of the overall power supply of the system. The fault downtime refers to the interruption time from the occurrence of the fault to the completion of the location and the start of the recovery process. The load recovery efficiency refers to the proportion of the load restored per unit time to the total load, which is used to measure the speed and effectiveness of the recovery process. The experiment is based on the results of multiple medium-voltage cable fault simulations, and the average performance of different methods is statistically analyzed. The results are shown in Table 4.

Table 4. System recovery time and fault downtime of different methods, load recovery efficiency.

Methods	System recovery time (s)	Fault downtime (s)	Load recovery efficiency (%)
TW method	13.6	8.9	81.2
Impedance method	15.3	9.7	78.4
BP	10.2	6.5	85.9
CSA-WNN	7.4	4.3	90.3
WNN	8.1	4.9	88.5
GA-PSO-WNN (adaptive wavelet basis)	6.2	3.7	93.6

In Table 4, from the perspective of system recovery time and fault downtime, the GA-PSO-WNN (adaptive wavelet basis) method performs best, with a system recovery time of only 6.2s and a fault downtime of 3.7s. The recovery time of the traditional TW method is 13.6s and the downtime is 8.9s, while the impedance method is 15.3s and 9.7s respectively. The BP neural network method has a significant improvement over the traditional method, with a system recovery time of 10.2s and a downtime of 6.5s. The system recovery time and fault downtime of the ordinary WNN are 8.1s and 4.9s respectively, while the CSA-WNN only takes 7.4s and 4.3s. It shows that with the intelligence of the algorithm and the optimization of the structure, the fault location accuracy is higher and the response is faster, which effectively reduces the interruption time of the cable system.

In terms of load recovery efficiency, GA-PSO-WNN takes the lead with an efficiency of 93.6%. CSA-WNN and WNN are 90.3% and 88.5% respectively, and the BP method is 85.9%. The traditional TW method and impedance method have low load recovery efficiency, which are 81.2% and 78.4% respectively. High load recovery efficiency means that more electricity consumption is restored per unit time, which is of great significance to the operation continuity of the power system and the user-side experience. It can be seen that the more advanced the optimization algorithm, the more it can improve the recovery ability of the power supply system after a sudden failure.

Traditional methods such as the TW method and the impedance method are easily affected by interference signals in complex environments, resulting in large positioning errors and long processing times. Algorithms based on neural networks, such as BP and WNN, have certain learning capabilities, but are prone to falling into local optimality and have weak generalization capabilities. After introducing improved mechanisms such as CSA or GA-PSO (adaptive wavelet basis), the model's ability to extract signal features and parameter adaptability are significantly enhanced. In particular, GA-PSO-WNN combines the multi-scale feature extraction capability of the adaptive wavelet basis, which can more accurately identify fault points and avoid falling into local optimality. At the same time, it can effectively shorten downtime and achieve large-scale load recovery in the shortest time, achieving high-efficiency and high-reliability fault location and system recovery.

H. Comparison Results with Other Deep Learning Methods

In order to further verify the feasibility of the GA-PSO-WNN (adaptive wavelet basis) method, a comparative experiment was conducted in an environment with a cable length of 100 km. The results are shown in Figure 8. In Figure 8, the comparison models include 1DCNN-BSVM, CNN-LSTM, BiGRU-ResNet, DSCNN-SA-SE, and BiLSTM.

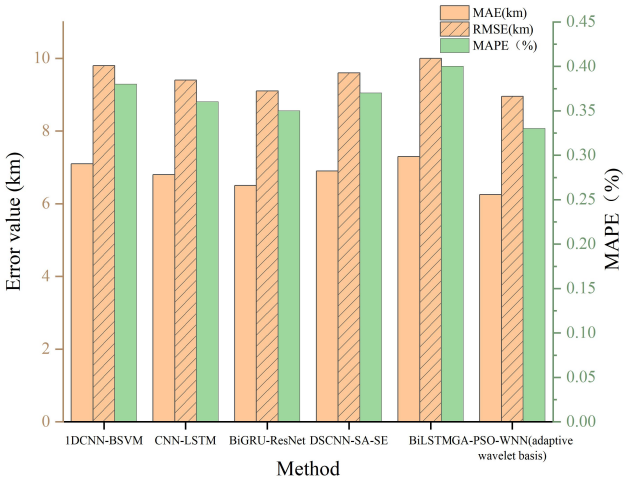

Figure 8. Comparison results with other deep learning methods.

In Figure 8, for *MAE* and *RMSE*, GA-PSO-WNN (adaptive wavelet basis) performs best, with *MAE* of 6.25 km and RMSE of 8.95 km. Other methods such as BiLSTM and 1DCNN-BSVM perform relatively poorly with MAE of 7.3 km and 7.1 km, *RMSE* of 10.0 km and 9.8 km, respectively. The *MAE* s of CNN-LSTM, BiGRU-ResNet and DSCNN-SA-SE are 6.8 km, 6.5 km and 6.9 km, respectively, which are also higher than GA-PSO-WNN, indicating that GA-PSO-WNN has more advantages in positioning accuracy and stability.

In terms of *MAPE*, GA-PSO-WNN still performs best, only 0.33%. The *MAPE* of other models such as BiLSTM and 1DCNN-BSVM are 0.40% and 0.38% respectively, with relatively large relative errors, while the *MAPE* of CNN-LSTM, BiGRU-ResNet, and DSCNN-SA-SE are 0.36%, 0.35%, and 0.37% respectively.

GA-PSO-WNN introduces GA and PSO to jointly optimize network parameters, so that the model can jump out of the local optimum and find a more global solution.

Moreover, the WNN structure using adaptive wavelet basis can more flexibly capture the non-stationary characteristics in the cable fault reflection signal. Compared with the traditional convolutional network or RNN structure, it has stronger local time-frequency analysis ability for the signal, which improves the accuracy of positioning. Although other models such as BiLSTM and CNN-LSTM have advantages in time series modeling, they may not achieve the optimal expression of features or parameter tuning, resulting in relatively large errors. In particular, the combined model of 1DCNN-BSVM has bottlenecks in nonlinear feature extraction, and its accuracy is more obviously limited. In summary, GA-PSO-WNN shows stronger performance advantages in cable fault location tasks due to its optimization strategy and signal adaptability design.

I. Convergence Stability Analysis

To further verify the convergence stability, this paper repeats the GA-PSO-WNN (adaptive wavelet basis) and the comparison method 10 times under the same 100km cable condition, and counts the fitness value and convergence iteration number at the end of each final iteration, and calculates the mean and standard deviation. The results are shown in Table 5.

Table 5.

Method	Average final fitness (mean±std)	Average number of convergence iterations (mean±std)
GA-PSO-WNN (adaptive wavelet basis)	0.925 ± 0.003	72 ± 4
PSO- WNN	0.887 ± 0.005	61 ± 6
GA- WNN	0.855 ± 0.007	92 ± 8
CSA- WNN	0.851 ± 0.010	101 ± 9
SSA- WNN	0.882 ± 0.006	82 ± 7

In Table 5, for the average final fitness, GA-PSO-WNN (adaptive wavelet basis) leads all methods with a score of 0.925±0.003, which is significantly better than PSO-WNN's 0.887±0.005 and SSA-WNN's 0.882±0.006. GA-WNN reaches 0.855±0.007 and CSA-WNN reaches 0.851±0.010, which is more average. The results show that GA-PSO-WNN finds higher quality parameter combinations overall, with lower training error and better model fit.

In terms of the average number of convergence iterations, PSO-WNN is the fastest, reaching stability in only 61±6 iterations, followed by GA-PSO-WNN with 72±4 times, SSA-WNN and GA-WNN require 82±7 and 92±8 times respectively, and CSA-WNN is the slowest, reaching 101±9 times. Although PSO-WNN has an advantage in convergence speed, its fitness level is still far behind that of GA-PSO-WNN, while GA-PSO-WNN achieves the best balance between speed and effect.

GA-PSO-WNN adopts a serial fusion optimization strategy. The GA stage is responsible for extensive exploration of the parameter space to avoid falling into the local optimum in the early stage, while the PSO stage conducts a refined search in the excellent area of GA output, so that the model can eventually converge to a higher fitness value. At the same time, the adaptive wavelet basis selection provides a more representative feature expression for the network, improves the "signal quality" of the optimization process, and further improves the upper limit and stability of the final fitness. Although PSO-WNN can quickly complete the search using inertia weights and individual/global optimal information, it lacks global diversity guarantees, resulting in early convergence but difficulty in further improvement. On the contrary, pure GA-WNN has a strong global exploration ability but is not efficient in detail tuning, so it converges slowly. The construction of CSA-WNN introduces diversified search, but its update mechanism does not provide enough detailed mining of local areas, which slows down the speed and makes it difficult to converge to the optimal point. This paper connects GA and PSO in series and supplements them with adaptive feature selection, which is the key to achieving high fitness and fast and stable convergence.

J. Friedman Test and Wilcoxon Signed Rank Test

To further evaluate the statistically significant differences in fault location accuracy among different algorithms, this paper uses the Friedman test and Wilcoxon signed rank test for analysis. The compared algorithms include: GA-PSO-WNN, PSO-WNN, GA-WNN, CSA-WNN, SSA-WNN, 1DCNN-BSVM, CNN-LSTM, BiGRU-ResNet, DSCNN-SA-SE, BiLSTM.

Under the same 100km cable condition, all algorithms were run 10 times each, and the final fitness values were recorded as statistical samples. The Friedman test is used to determine whether there are significant differences among all algorithms as a whole; the Wilcoxon test is used for further pairwise comparisons to determine which specific algorithms have significant differences. The statistical results of the Friedman test are shown in Table 6.

Table 6. Statistical results of the Friedman test.

Method	Average rank	$x^2(9)$	p value
GA-PSO-WNN	1.3	61.47	<0.001
PSO-WNN	2.9		
BiGRU-ResNet	3.7		
DSCNN-SA-SE	4.1		
BiLSTM	4.5		
SSA-WNN	5.1		
GA-WNN	6.1		
CNN-LSTM	6.3		
1DCNN-BSVM	7.1		
CSA-WNN	8		

From the statistical results of the Friedman test in Table 6, it can be seen that the average ranking differences of all algorithms are quite obvious. GA-PSO-WNN ranks the highest, with an average ranking of 1.3, indicating that the algorithm performs best in fault location accuracy and is significantly better than other algorithms. The average ranking of PSO-WNN is 2.9, and the average ranking of BiGRU-ResNet is 3.7. CSA-WNN ranks the lowest, with an average ranking of 8, indicating that the algorithm is relatively poor in accuracy.

According to the P value of the Friedman test (<0.001), it can be seen that the location accuracy differences between different algorithms are statistically significant. The P value is much smaller than the significance level of 0.05 usually set, indicating that in the task of fault location, there are significant differences in the performance of each algorithm, and further pairwise comparisons are needed to determine which specific algorithms have significant differences.

The results of the Wilcoxon signed rank test are shown in Table 7.

Table 7. Wilcoxon signed rank test results.

GA-PSO-WNN vs other	Z value	p value	Significance judgment $(\alpha = 0.05)$
PSO-WNN	-2.401	0.013	Significant differences
GA-WNN	-2.712	0.008	
CSA-WNN	-2.897	0.005	
SSA-WNN	-2.406	0.016	
1DCNN-BSVM	-2.221	0.022	
CNN-LSTM	-2.687	0.009	
BiGRU-ResNet	-2.09	0.036	
DSCNN-SA-SE	-2.035	0.041	
BiLSTM	-2.328	0.019	

In the Wilcoxon signed rank test results in Table 7, the differences in fault location accuracy between GA-PSO-WNN and other algorithms have reached a significant level $(\alpha = 0.05)$. The Z value of GA-PSO-WNN and PSO-WNN is -2.401, the p value is 0.013, the Z value of GA-PSO-WNN and GA-WNN is -2.712, the p value is 0.008, the Z value of GA-PSO-WNN and CSA-WNN is -2.897, the p value is 0.005, and the Z value of GA-PSO-WNN and SSA-WNN is -2.406, the p value is 0.016. It can be seen that the differences between the algorithms are significant. This shows that GA-PSO-WNN has obvious advantages in these algorithms and can provide higher positioning accuracy.

The Z value of GA-PSO-WNN and 1DCNN-BSVM is -2.221, the p value is 0.022, the Z value of GA-PSO-WNN and 1DCNN-BSVM is -2.687, the p value is 0.009, and the Z value of GA-PSO-WNN and BiGRU-ResNet is -2.09, the p value is 0.036. The Z value of GA-PSO-WNN and DSCNN-SA-SE is -2.035, the p value is 0.041, and the Z value of GA-PSO-WNN and BiLSTM is -2.328, the p value is 0.019, which further verifies the relative advantages of GA-PSO-WNN among multiple algorithms and shows the strong ability and stability of this method in fault location tasks.

6. Experimental Discussion

The experimental results of this paper show that by introducing adaptive wavelet basis, GA and PSO optimization algorithm, the improved GA-PSO-WNN (adaptive wavelet basis) in this paper shows obvious

advantages in cable fault location. This result is mainly due to several factors: the introduction of adaptive wavelet basis can effectively process high-frequency details and instantaneous changes in the signal, improve the feature extraction ability of fault signal, and optimize the learning effect of the network. GA and PSO algorithms fine-tune network parameters such as scaling factor, translation factor and network weight through global and local joint optimization, thus overcoming the problem that traditional WNN is prone to fall into local optimality and improving the positioning accuracy and robustness of the model. Compared with other methods, the TW method and impedance method are overly dependent on a single signal feature, resulting in poor adaptability under complex signal conditions, while the BP network is prone to unstable prediction results due to the use of gradient descent optimization, which further verifies the advantages of the GA-PSO-WNN (adaptive wavelet basis) method.

The improved GA-PSO-WNN (adaptive wavelet basis) method in this study has important application significance in cable fault location. The method combines the swarm intelligence optimization algorithm GA and PSO, as well as advanced signal processing technology, breaking the bottleneck of poor adaptability and low accuracy of traditional fault location methods in complex environments. This paper uses the improved wavelet basis with strong adaptability to better cope with the complexity and uncertainty of cable signals, providing a more accurate and real-time responsive solution for fault location in power systems. This study also provides new ideas for signal processing and fault detection in similar fields, and promotes the application of neural networks based on intelligent optimization, which has important theoretical value and practical significance.

The GA-PSO-WNN (adaptive wavelet basis) method has good generalization ability and can be applied to fault location of overhead lines or hybrid lines. The key advantage of this method is that it uses MI-driven adaptive wavelet basis selection to dynamically select the optimal wavelet basis function according to the characteristics of different line signals, and adapt to the strong reflection signals, interference noise and nonlinear waveform changes in overhead lines. At the same time, through the hybrid optimization strategy of GA and PSO, the WNN parameters can be globally searched and fine-tuned to improve the model's ability to identify and locate complex fault modes of overhead and hybrid lines. In practical applications, it is only necessary to collect the traveling wave signals of the corresponding lines and adapt the model input features, so that the method can be extended to the prediction of the distance to the fault point of overhead or hybrid lines, which is expected to achieve high-precision fault location for lines of several kilometers or even tens of kilometers.

In the GA-PSO-WNN cable fault location method of this paper, the neutral point grounding mode of the distribution system has an indirect but important impact on the performance and applicability of the algorithm. The neutral point grounding mode determines the current path and fault signal when a fault occurs in the cable system, especially the characteristics of the traveling wave signal, such as amplitude, duration, spectral components, etc. These characteristics directly affect the extraction quality of the traveling wave signal and the expression effect of the wavelet feature. The GA-PSO-WNN method relies on the traveling wave signal for feature extraction, optimal wavelet basis selection and neural network training. Therefore, different grounding modes, such as direct grounding, grounding through arc suppression coils, and no grounding, may lead to significant differences in the time-frequency characteristics of the fault signal, affecting the mutual information-driven wavelet basis adaptive selection results and the training accuracy of the WNN. In practical applications, the traveling wave characteristic analysis and model parameter tuning should be carried out for specific grounding modes to ensure the accuracy and robustness of the GA-PSO-WNN model.

The improved WNN method in this paper performed well in the experiment, but there are still some limitations. Future research can be improved and expanded in the following aspects:

(1) The experiment in this paper is mainly aimed at fault location of cables with a length of 100km to 800km, which is limited in scope. In the future, it can be extended to cables with longer distances, and more complex cable network topologies and various types of faults can be considered for more comprehensive verification.

(2) The method in this paper has strong anti-noise ability, but the positioning error still increases in a high-intensity noise environment. In the future, time-frequency analysis or multi-sensor data fusion can be combined to further improve the system's adaptability to complex interference.

(3) With the development of deep learning technology, WNN can be improved in the future by combining deep technologies such as convolutional neural networks to achieve more accurate and rapid fault location, further improving the real-time and intelligent level of the system.

7. Conclusions

This paper adopts a medium voltage cable fault point location method based on improved WNN. By introducing the MI driven wavelet basis adaptive selection mechanism and combining the GA-PSO algorithm, multiple key parameters of WNN are jointly optimized, which effectively improves the accuracy of fault point location and the convergence efficiency of the model. Experimental results show that this method shows good positioning performance and robustness under different cable lengths and noise intensity conditions. Compared with the traditional WNN, the improved model has significant optimization in MAE,

RMSE and convergence speed, reducing the error by 1.95km and 2.25km respectively. This study has made some achievements, but there are still some limitations. The diversity of fault types and cable lengths is relatively narrow and not fully covered. Moreover, this paper is based on simulation experiments and cannot be verified in experimental scenarios. In the future, it can be expanded to a wider range of cable scenarios and experiments can be conducted in actual cable detection scenarios. At the same time, multimodal fusion and deep learning technologies can be introduced to further improve the generalization ability and intelligence level of WNN.

Acknowledgment

None

Consent to Publish

The manuscript has neither been previously published nor is under consideration by any other journal. The authors have all approved the content of the paper.

Funding

State Grid Fujian Electric Power Co., LTD. Science and Technology Project Detection of Latent Faults in Low-Current Grounding Systems Based on Composite Criteria. (No. SGFJFZ00PDJS2311041)

Author Contribution

[Yibiao Huang, Wenxuan Xu]: Developed and planned the study, performed experiments, and interpreted results. Edited and refined the manuscript with a focus on critical intellectual contributions.

[Yirong Ye, Xiaoqiang Wen]: Participated in collecting, assessing, and interpreting the date. Made significant contributions to date interpretation and manuscript preparation.

[Xiong Chen, Yunxiang Xu]: Provided substantial intellectual input during the drafting and revision of the manuscript.

Conflicts of Interest

The authors declare that they have no financial conflicts of interest.

References

[1] A. Achitaev, K.V. Suslov, I.O. Volkova, V.E. Kozhemyakin, Y.V. Dvoryansky. Development of an algorithm for identifying single-phase ground fault conditions in cable and overhead lines in the networks with isolated neutral. Energy Reports, 2023, 9(1), 1079-1086. DOI: 10.1016/j.egyr.2023.01.046

[2] M.H. Saad, A. Said. Machine learning-based fault diagnosis for research nuclear reactor medium voltage power cables in fraction Fourier domain. Electrical Engineering, 2023, 105(1), 25-42. DOI: 10.1007/s00202-022-01649-7

[3] S.B. Li, B.L. Cao, J. Li, Y. Cui, Y.Q. Kang, G.N. Wu. Review of condition monitoring and defect inspection methods for composited cable terminals. High Voltage, 2023, 8(3), 431-444. DOI: 10.1049/hve2.12318

[4] Y. Li, L.Y. Jiang, M. Xie, J. Yu, L. Qian, K. Xu, et al. Advancements and challenges in power cable laying. Energies, 2024, 17(12), 2905-2930. DOI: 10.3390/en17122905

[5] W.S. Cao, L.X. Zhao, Z.H. Li, J.M. Chen, M.M. Xu, R.Z. Niu. Fault Location Study of Overhead Line–Cable Lines with Branches. Processes, 2023, 11(8), 2381-2409. DOI: 10.3390/pr11082381

[6] J.J. Liu, M.C. Ma, X. Liu, H.K. Xu. High-Voltage Cable Buffer Layer Ablation Fault Identification Based on Artificial Intelligence and Frequency Domain Impedance Spectroscopy. Sensors, 2024, 24(10), 3067-3086. DOI: 10.3390/s24103067

[7] S.R. Li, B.R. Gu, X.G. Zhu, H. Li, J..B. Deng, G.J. Zhang. High impedance grounding fault location method for power cables based on reflection coefficient spectrum. Energy Reports, 2023, 9(1), 576-583. DOI: 10.1016/j.egyr.2023.01.066

[8] X. Chen, Q.S. Guan, Q.X. Guan, X. Jin, Z. Shi. A wavenumber domain reflectometry approach to locate and image line-like soft faults in cables. IEEE Transactions on Instrumentation and Measurement, 2023, 72(1), 1-12. DOI: 10.1109/TIM.2023.3322999

[9] G.Q. Sun, W. Ma, S.Q. Wei, D.F. Cai, W.Z. Wang, C.Z. Xu, et al. A Fault Location Method for Medium Voltage Distribution Network Based on Ground Fault Transfer Device. Electronics, 2023, 12(23), 4790-4802. DOI: 10.3390/electronics12234790

[10] R.C. Zeng, L.L. Zhang, Q.H. Wu. Fault location scheme for multi-terminal transmission line based on frequency-dependent traveling wave velocity and distance matrix. IEEE Transactions on Power Delivery, 2023, 38(6), 3980-3990. DOI: 10.1109/TPWRD.2023.3293998

[11] Bugajska, T. Desaniuk. Impedance-based short circuit-Short circuit fault location method in coaxial cables. IEEE Access, 2023, 11(1), 115231-115279. DOI: 10.1109/ACCESS.2023.332064

[12] J.G. Su, L.Q. Wei, P. Zhang, Y. Li, Y.P. Liu. Multi-type defect detection and location based on non-destructive impedance spectrum measurement for underground power cables. High Voltage, 2023, 8(5), 977-985. DOI: 10.1049/hve2.12331

[13] Q.Z. Wan, Y.M. Li, R.J. Yuan, Q.H. Meng, X.X. Li. Fault identification and localization of a time− frequency domain joint impedance spectrum of cables based on deep belief networks. Sensors, 2023, 23(2), 684-700. DOI: 10.3390/s23020684

[14] S.H.A. Niaki, J.S. Farkhani, Z. Chen, B. Bak-Jensen, S.J. Hu. An Intelligent Method for Fault Location Estimation in HVDC Cable Systems Connected to Offshore Wind Farms. Wind, 2023, 3(3), 361-374. DOI: 10.3390/wind3030021

[15] Hadaeghi, M.M. Iliyaeifar, A.A. Chirani. Artificial neural network-based fault location in terminal-hybrid high voltage direct current transmission lines. International Journal of Engineering, 2023, 36(1), 215-225. DOI: 10.5829/IJE.2023.36.02B.03

[16] Z.G. Shang, Z.B. Zhao, R.Q. Yan. Denoising fault-aware wavelet network: A signal processing informed neural network for fault diagnosis. Chinese Journal of Mechanical Engineering, 2023, 36(1), 9-26. DOI: 10.1186/s10033-023-00838-0

[17] X.U. Xianfeng, M.A. Zhixiong, Y.A.O. Jingjie, L.I.

Zhihan, W. Ke. Cable Fault Location Based on Wavelet Transform and GA-BP Neural Network. Journal of Electrical Engineering, 2024, 19(2), 146-155. DOI: 10.11985/2024.02.017

[18] Y.N. Tao. Three-dimensional simulation and localization of power cable fault point by combining wavelet transform and neural network. 3c Tecnología: Glosas de Innovación Aplicadas a La Pyme, 2024, 13(1), 35-55. DOI: 10.17993/3ctecno.2024.v13n1e45.35-55

[19] Zhou, S.Y. Gui, Y. Liu, J.P. Ma, H. Wang. Fault location of distribution network based on back propagation neural network optimization algorithm. Processes, 2023, 11(7), 1947-1960. DOI: 10.3390/pr11071947

[20] X. Hu, N. Pang, H.B. Guo, R. Wang, F. Li, G. Li. Research on RTD Fluxgate Induction Signal Denoising Method Based on Particle Swarm Optimization Wavelet Neural Network. Sensors, 2025, 25(2), 482-497. DOI: 10.3390/s25020482

[21] P. Ong, Z. Zainuddin. An optimized wavelet neural networks using cuckoo search algorithm for function approximation and chaotic time series prediction. Decision Analytics Journal, 2023, 6(10), 1-12. DOI: 10.1016/j.dajour.2023.100188

[22] S. Baroumand, A.R. Abbasi, M. Mahmoudi. Integrative fault diagnostic analytics in transformer windings: Leveraging logistic regression, discrete wavelet transform, and neural networks. Heliyon, 2025, 11(4), 1-16. DOI: 10.1016/j.heliyon.2025.e42872

[23] S. Altaie, A.A. Majeed, M. Abderrahim, A. Alkhazraji. Fault detection on power transmission line based on wavelet transform and scalogram image analysis. Energies, 2023, 16(23), 7914-7932. DOI: 10.3390/en16237914

[24] N. Ahmed, A.A. Hashmani, S. Khokhar, M.A. Tunio, M. Faheem. Fault detection through discrete wavelet transform in overhead power transmission lines. Energy Science & Engineering, 2023, 11(11), 4181-4197. DOI: 10.1002/ese3.1573

[25] S.R.K. Joga, P. Sinha, V. Manoj, S.R. Sura, V.N. Pudi, N.F. Ibrahim, et al. Applications of tunable-Q factor wavelet transform and AdaBoost classier for identification of high impedance faults: Towards the reliability of electrical distribution systems. Energy Exploration & Exploitation, 2024, 42(6), 2017-2055. DOI: 10.1177/01445987241260949

[26] L. Huang, X.Q. Zhou, L.H. Shi, L. Gong. Time Series Feature Selection Method Based on Mutual Information. Applied Sciences, 2024, 14(5), 1960-1973. DOI: 10.3390/app14051960

[27] G. Gowri, X.K. Lun, A. Klein, P. Yin. Approximating mutual information of high-dimensional variables using learned representations. Advances in Neural Information Processing Systems, 2024, 37(1), 132843-132875. DOI: 10.48550/arXiv.2409.02732

[28] Y.A. Ali, E.M. Awwad, M. Al-Razgan, A. Maarouf. Hyperparameter search for machine learning algorithms for optimizing the computational complexity. Processes, 2023, 11(2), 349-369. DOI: 10.3390/pr11020349

[29] J. Japa, M. Serqueira, A.I. Mendonc, M. Aritsugi, E. Bezerra, P.H. Gonzalez. A population-based hybrid approach for hyperparameter optimization of neural networks. IEEE Access, 2023, 11(1), 50752-50768. DOI: 10.1109/ACCESS.2023.3277310

[30] F.Z. El-Hassani, M. Amri, N.E. Joudar, K. Haddouch. A new optimization model for MLP hyperparameter tuning: modeling and resolution by real-coded genetic algorithm. Neural Processing Letters, 2024, 56(2), 105-135. DOI: 10.1007/s11063-024-11578-0

[31] T. Cansu, E. Kolemen, O. Karahasan, E. Bas, E. Egrioglu. A new training algorithm for long short-term memory artificial neural network based on particle swarm optimization. Granular Computing, 2023, 8(6), 1645-1658. DOI: 10.1007/s41066-023-00389-8

[32] Y.Y. Hong, L.F. Chen, W. Zhang. Classification of photovoltaic faults using PSO-optimized compact convolutional transformer. IEEE Access, 2023, 11(1), 140752-140762. DOI: 10.1109/ACCESS.2023.3341889

[33] R. Abdulkadirov, P. Lyakhov, N. Nagornov. Survey of optimization algorithms in modern neural networks. Mathematics, 2023, 11(11), 2466-2502. DOI: 10.3390/math11112466

[34] M. Reyad, A.M. Sarhan, M. Arafa. A modified Adam algorithm for deep neural network optimization. Neural Computing and Applications, 2023, 35(23), 17095-17112. DOI: 1007/s00521-023-08568-z

[35] Zhang, Y.C. Shao, H.J. Sun, L. Xing, Q. Zhao, L. Zheng. The WuC-Adam algorithm based on joint improvement of Warmup and cosine annealing algorithms. Mathematical Biosciences and Engineering, 2024, 21(1), 1270-1285. DOI: 10.3934/mbe.2024054 Previous Article Next Article